SMEARED CRACK APPROACHES—MATERIAL MODELING

By Marco Petrangeli[1] and Joško Ožbolt[2]

ABSTRACT: Since the smeared crack concept has proved to be very attractive when used in the finite-element fracture analysis, many different material models have been put forward. The majority of these models, usually known as a single or multiple crack models, are based on a linear elastic material constitutive law coupled in series with a softening crack-bridging law. The crack-bridging law on the plane where tensile fracture occurs, although defined in terms of stresses and strains, is basically the same vectorial relation used in the discrete crack approach. These models yield some problems due to the nonconsistency of the basic hypothesis and sharp discontinuities in the resulting material behavior. In this paper some of these problems are analyzed and compared with concepts and results coming from the nonlocal microplane material model. Numerical studies on the material and finite-element level using both approaches are reported.

INTRODUCTION

In the macroscopical finite-element fracture analysis of quasibrittle materials such as concrete, two approaches are currently in use: (1) Discrete crack approach; (2) smeared crack approach. In the discrete crack approach, besides a realistic macroscopical material model, a crack-bridging law for discrete crack has to be used. The main disadvantage of this approach is that continuous remeshing is required, which in three-dimensional finite-element analysis as well as in the case of multiple crack situations significantly slow down the efficiency of the method. Therefore, in order to overcome the problem of remeshing, alternatively, the smeared crack approach has been introduced.

The basic requirement for the smeared crack finite-element analysis of a concrete structure is that the analysis must not exhibit mesh sensitivities. However, using most of the current smeared cracked finite-element codes one can observe two types of mesh sensitivities: (1) Mesh sensitivity with respect to the shape (orientation) of the finite elements; and (2) mesh sensitivity with respect to the size of the elements. The second kind of sensitivity can be effectively overcome only by using a nonlocal approach. However, the mesh shape (orientation) sensitivity seems to strongly depend on the local material constitutive law employed in the analysis. Nonetheless, recent development in the nonlocal approaches (Ožbolt and Bažant 1994) also indicated the shape sensitivity as long as the local material behavior itself is not prone to the stress locking phenomena.

In current smeared computational fracture analysis, beside continuous material models (microplane models, plasticity models with degrading yield surface, and others) single or multicrack models are very popular (de Borst and Nauta 1985; de Borst 1987; Rots 1988). Using these models one can observe strong mesh shape sensitivity (Rots 1992). In fact, it seems that these models are generally not applicable in the smeared crack analysis without continuous remeshing, except if the crack pattern is known in advance. Therefore, to understand and explain in more detail what the main reasons for significant mesh shape sensitivity are, in this paper the fixed crack material model, which exhibits strong mesh shape sensitivity, is compared with the microplane model, which shows a much better behavior with regard to the mesh shape sensitivity problem.

[1]Res. Engr., Institut für Werkstoffe im Bauwesen, Stuttgart University, Germany.

[2]Res. Engr., Institut für Werkstoffe im Bauwesen, Stuttgart University, Germany.

Note. Associate Editor: P. K. Banerjee. Discussion open until November 1, 1996. To extend the closing date one month, a written request must be filed with the ASCE Manager of Journals. The manuscript for this paper was submitted for review and possible publication on December 1, 1993. This paper is part of the ***Journal of Engineering Mechanics***, Vol. 122, No. 6, June, 1996. ©ASCE, ISSN 0733-9399/96/0006-0545–0554/ $4.00 + $.50 per page. Paper No. 7466.

MATERIAL MODEL REVIEWS

Single Fixed Crack Approach

When the single crack approach was introduced into the smeared crack finite-element analysis (Bažant and Oh 1983), fixed crack must have been regarded as the natural evolution of the discrete crack approach. In the single fixed crack approach a linear elastic material tensor is coupled via a static constraint with a local matrix, which describes the softening crack-opening relation. This behavior is defined on the principal tensile plane and, although the principal stresses may rotate during the analysis, the orientation of this plane is fixed in the direction where trespassing of tensile resistance occurred first. Physical support for this was possibly found in macrocracking where the crack, due to the complete loss of material resistance, cannot rotate.

In the following paragraphs a brief overview of the single smeared crack approach is given with all the examples and mathematical expressions referred to the plane stress analysis. Since on the crack plane only two stress and strain components have physical meaning [normal n and shear t—see Fig. 1(a)], the crack stress increment tensor $\Delta\sigma_{cr}$ reads

$$\Delta\sigma_{cr} = (\Delta\sigma_n \Delta\sigma_t) \tag{1}$$

Calling $n = (n_x n_y)$ the unit vector normal to the crack plane; and $t = (t_x t_y)$ the tangent one, the transformation matrix $\mathbf{N}_{cr}$ between global and local crack coordinate systems is

$$\mathbf{N}_{cr} = \begin{pmatrix} n_x^2 & n_y^2 & 2n_x t_x \\ n_x n_y & t_x t_y & n_x t_y + n_y t_x \end{pmatrix} \tag{2}$$

The basic concept of the single smeared crack approach is then summarized in the following:

$$\Delta\sigma_{cr} = \mathbf{N}_{cr} \Delta\sigma \tag{3}$$

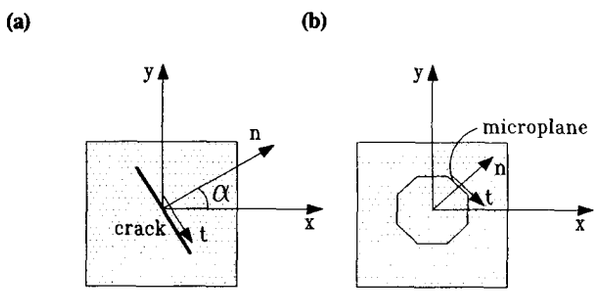

FIG. 1. Treatment of Cracks in: (a) Single Crack Approach; (b) Microplane Material Model

According to (3) the projection of the global stress tensor on the crack plane must be in equilibrium with the crack stresses. To assemble the material stiffness matrix, a linearized stress-strain relation for the crack plane is needed in the following form:

$$\Delta\sigma_{cr} = \mathbf{K}^{cr}\Delta\mathbf{e}_{cr} \tag{4}$$

where $\mathbf{K}^{cr}$ = tangent stiffness matrix for the crack plane; and $\Delta\mathbf{e}_{cr} = (\varepsilon_n \varepsilon_t)$ the crack strain vector with normal and tangent components. Since the crack element is assembled in series with the elastic material (static constraint approach), the total strain vector $\Delta\varepsilon_{tot}$ is found as the sum of the elastic strain $\Delta\varepsilon_{el}$ and the crack strain $\Delta\varepsilon_{cr}$. The crack strain is written in the local crack coordinate system, therefore, it needs to be transformed in global directions. Using the transformation matrix $\mathbf{N}_{cr}$, the following expression is found:

$$\Delta\varepsilon_{tot} = \Delta\varepsilon_{el} + \mathbf{N}_{cr}^{T}\Delta\mathbf{e}_{cr} \tag{5}$$

where $\Delta\varepsilon_{cr} = \mathbf{N}_{cr}^{T}\Delta\mathbf{e}_{cr}$. Calling $\mathbf{K}^{el}$ the stiffness matrix of the linear elastic material, the resulting tangent stiffness matrix $\mathbf{K}^{tot}$ of the cracked material can be written as (Rots 1988)

$$\mathbf{K}^{tot} = \mathbf{K}^{el} - \mathbf{K}^{el}\mathbf{N}_{cr}^{T}(\mathbf{K}^{cr} + \mathbf{N}_{cr}\mathbf{K}^{el}\mathbf{N}_{cr}^{T})^{-1}\mathbf{N}_{cr}\mathbf{K}^{el} \tag{6}$$

This method of assembling the material stiffness matrix is very much a derivative of the discrete crack approach. The resulting matrix is a modification of the elastic matrix by a smaller rank one. Since no integration is involved over the material volume (different orientations), the crack plane causes an immediate sharp anisotropy in the material, which does not seem to happen in physical experience. It is indeed very unlikely that the damage should be localized from the very beginning (after the tensile strength is reached) on a determined orientation from which no deviation or range is explicitly accounted for.

A typical form used for stiffness crack matrix in plane stress is (Rots 1988)

$$\mathbf{K}^{cr} = \begin{pmatrix} \dfrac{\mu}{1-\mu}E & 0 \\ 0 & \dfrac{\beta}{1-\beta}G \end{pmatrix} \tag{7}$$

In this way the normal and sliding crack opening relations (mode I and mode II, respectively) are related to the elastic stiffness via two coefficients. The first coefficient μ, for mode I behavior, is negative and accounts for the softening branch of the stress-strain curve. The second coefficient β is the so-called shear retention factor. At crack initiation it must satisfy the condition $0 < \beta \leq 1$, since the crack opening is based on a threshold value for either principal stress or strain. Shear stress at crack initiation on the crack plane is zero and any increment of shear strain on this plane must yield to a non-negative stress. Later in the analysis, the shear stiffness may become negative (softening) and the shear stresses released, the same as in the mode-I fracture.

Setting β to zero yields a zero stiffness value for the correspondent component in $\mathbf{K}^{cr}$. This means that there is no shear resistance in the crack plane and it remains the principal plane for stresses but not for strains. For any other value of β the principal axes for strains and stresses rotate, generally, losing coaxiality. Any value of β different from zero means that a portion of the elastic shear stiffness is retained. This finds its physical background in aggregate interlock. However, in numerical analysis it causes a problem due to the severe stress locking, which results in a strong mesh shape sensitivity.

When using expression (7), the two parameters μ and β do not interact with each other. An explicit interaction between the two should be found via an expression for the off-diagonal terms in the crack matrix (7). This was perceived to be too complicated and, therefore, an implicit relation is usually used by which β depends on the strain normal to the crack plain (ε_1^{cr}) as

$$\beta = \left(1 - \frac{\varepsilon_1^{cr}}{\varepsilon_u^{cr}}\right)^{p} \tag{8}$$

where ε_u^{cr} = strain value at the moment when the microcracks coalesce into a continuous macrocrack; and p = a positive constant larger than zero. In (8) β is decreasing when increasing the crack width according to the power law, which from physical experience seems logical.

Multidirectional Fixed Crack Approach

The multidirectional fixed crack approach is based on the same assumptions as the single fixed crack approach. The possibility of having a multiple crack plane gives more accuracy when stresses are rotating due to change in the load pattern or shift in the principal stress directions. The material behavior is found from coupling multiple planes, each representing a different crack orientation with a linear elastic material (de Borst and Nauta 1985). Every single crack plane holds what has been said for the single fixed crack approach. After the first crack initiates, the following crack plane initializations are decided on the trespassing of a threshold value in intensity and/or orientation. Criteria for this can be optimized based on computer resources and numerical accuracy needed.

The multidirectional fixed crack approach does not overcome the problems arising from the inconsistency of the material model already mentioned for the single crack model. The presence of multiple planes does not give rise to a different assembling for the stiffness matrix and resultant material model. The advantage of the multiple approach against the single fixed crack approach, with respect to the stress locking, must be found in the possibility of releasing energy on new crack initializations. As a matter of fact this possibility is only theoretical, since, in finite elements the internal redundancy of the strain field is such that highly distorted stress fields can still retain most of the locked energy with the multiple crack plane option, as will be shown in the numerical examples.

Rotating Crack Approach

To overcome the problem of stress locking and mesh sensitivity, the rotating crack concept has been developed (Cope et al. 1980; Rots 1988) in which the crack always orientated normal to the principal tensile stress. In this way the system cannot rebuild tensile stresses without the crack plane chasing and releasing it. The assembly of the material stiffness matrix is identical to that shown for the fixed crack approach. The only difference is in the coordinate transformation matrix $\mathbf{N}_{cr}$, which is upgraded every load step, following the principal axes rotation. However, when nonlinear stress-strain relations are used the matrix $\mathbf{N}_{cr}$ must be iteratively upgraded inside the load step as well.

Although in the rotating crack models the crack plane is always perpendicular to the principal tensile stress, the coaxiality between principal stress and strain is generally lost. The problem can be overcome if arbitrariness of the shear retention factor is dropped and the resulting shear stiffness calculated imposes coaxiality of principal stress and strain (William et al. 1986; Crisfield and Willis, 1987). Rotating crack approaches based on this concept are known as "coaxial rotating crack models." Calling k_{33}^{tot}, the resulting shear stiffness of the matrix $\mathbf{K}^{tot}$, to enforce the coaxiality the following relation must satisfy (Bažant 1983):

$$k_{33}^{tot} = \frac{(\sigma_1 - \sigma_2)}{2(\varepsilon_1 - \varepsilon_2)} \tag{9}$$

where σ_1 = stress corresponding to the principal strain direction ε_1, which, due to softening in mode-I fracture, can be smaller than the σ_2 and thus yields a negative value for k_{33}^{tot}. This means that once the softening relation for mode-I fracture is fixed, the mode-II relation is automatically fixed as well. During the analysis negative value of β (shear softening behavior) can be found when fulfilling (9) (Rots 1988).

Microplane Material Model

In some respects similar to the multiple smeared crack approach is the microplane material model (Bažant and Prat 1988; Ožbolt and Bažant 1992). The model is assembled using a number of fixed planes [Fig. 1(b)] of various orientations, where simple uniaxial stress-strain relations are monitored. Memory of damage is easily stored since the monitoring planes do not change and the path dependency can be accounted for. A key difference between the microplane and the multiple smeared crack approach is in the way the strains on microplanes are found in the single or multiple crack approach. In the multicrack approach, once the global stresses are known the crack strains are found via equilibrium using the constitutive laws (3) and (4). There is no need to say that this procedure (static constraint approach) is cumbersome, especially when the softening crack-bridging law is to be coupled with plasticity-based material models instead of the linear elastic ones. On the contrary, in the microplane material model the microplane strains are the resolved components of the total macroscopic strain tensor (kinematic constrain approach). For an strain increment tensor $\Delta\varepsilon$, the corresponding strain increments on differently oriented microplanes are found as

$$\Delta\varepsilon_m = \mathbf{N}_m \Delta\varepsilon \tag{10}$$

When (10) is written in two-dimensional form, the transformation matrix $\mathbf{N}_m$ is of the same form as matrix $\mathbf{N}_{cr}$ (2) with direction cosines referred to the corresponding microplane's normal and tangent orientations [see Fig. 1(b)]. In this case the vector $\Delta\varepsilon_m = (\Delta\varepsilon_n \Delta\varepsilon_t)$ is also a two-component one, the same as in the crack approach. Using the kinematic constraint approach, the compatibility condition is satisfied automatically, and this is very helpful when the material behavior is to be followed in the softening regime.

In this paper the material behavior on each microplane is defined as follows:

$$\text{for } \varepsilon_n \geq 0\text{: } \sigma_n = C_N^0(1 - \omega_N)\varepsilon_n \tag{11}$$

$$\sigma_t = C_T^0(1 - \omega_T)\varepsilon_t \tag{12}$$

with

$$\omega_N = 1 - \exp\left[-\left(\frac{\varepsilon_n}{e_1}\right)^k\right] \tag{13}$$

$$\omega_T = 1 - \exp\left[-\left(\frac{\varepsilon_t}{e_2}\right)^r\right] \tag{14}$$

where e_1, e_2, k, and r = constants to be specified as input parameters for the model. If $\varepsilon_n \leq 0$ (compression) the linear elastic behavior is assumed. Once the stresses on microplanes are known, from known microplane strain components and microplane constitutive relations, the corresponding macrostress vector and the material stiffness matrix are found via the equality of the virtual work on the macro- (unit volume) and microplane (microplane surfaces) level, which for two-dimensions reads

$$\Delta\sigma^T\Delta\varepsilon = \int_S \Delta\sigma_m^T \Delta\varepsilon_m \, dS \tag{15}$$

Writing the stress-strain relation on the microplanes in tangent form

$$\Delta\sigma_m = \mathbf{K}^m\Delta\varepsilon_m + \Delta\rho_m \tag{16}$$

with $\Delta\rho_m$ = nonelastic stress increment vector; and $\mathbf{K}^m$ = tangent stiffness matrix given by the expression

$$\mathbf{K}^m = \begin{bmatrix} \dfrac{d\sigma_n}{d\varepsilon_n} & 0 \\ 0 & \dfrac{d\sigma_t}{d\varepsilon_t} \end{bmatrix} \tag{17}$$

On substituting (10) and (16) in (15) we can write for the macroscopic stress increment tensor

$$\Delta\sigma = \left[\int_S \mathbf{N}_m^T\mathbf{K}^m\mathbf{N}_m \, dS\right]\Delta\varepsilon + \int_S \mathbf{N}_m^T\Delta\rho \, dS \tag{18}$$

The approach is more efficient than the one used in the multiple smeared crack analysis since the computational costs are easily balanced by improved numerical behavior and speed of convergency. When monitoring constitutive laws on a certain number of planes (for example, in three-dimensional analysis 21 planes are usually used), it seems logical to assemble material behavior without having to rely on the elastic background media. This gives the possibility of modeling not only the fracture behavior, but also all major nonlinear phenomena in quasi-brittle materials. Further, the integration over the fixed set of microplanes also provides smoothness of the resulting model with respect to the interaction between off-diagonal terms in the material stiffness matrix.

The form of the Microplane material model that was presented earlier is, to say the least, very schematic. The stress-strain laws on the microplanes, which are in the more advanced version of the model (Ožbolt and Bažant 1992) defined using volumetric and deviatoric invariants, instead of the normal component, are not discussed at all and other features are just ignored.

LOCALIZATION LIMITERS

As already pointed out, in the finite-element fracture analysis one should distinguish the shape (orientation) and the mesh size sensitivities. The mesh shape sensitivity at the structural level has been claimed to have a solution in a correct nonlocal approach. However, the experience so far with the microplane model used together with the nonlocal microcrack interactions approach (Ožbolt and Bažant 1994) indicates the contrary, i.e., the shape mesh sensitivity cannot be avoided if the material model is inconsistent. Consistency and continuity of the material model ensures that the result of the nonlocal analysis does not depend on the mesh orientation and shape, as will be illustrated later on in a few numerical examples.

To prevent localization of damage into a zero volume, what is physically inadmissible and leads to the spurious mesh sensitivity [inobjectivity of the analysis with respect to the finite-element size; Bažant (1986)], the interaction at a distance between different particles of the material has to be somehow taken into account. This interaction is known as a localization limiter. Currently, in the finite-element codes there are two approaches: (1) Crack band approach; and (2) nonlocal approaches.

The crack band approach, introduced by Bažant and Oh (1983), prevents the localization of damage into a zero volume by modifying the stress-strain law such that the total fracture energy released in the cracked finite-element band should be a constant. In the approach the problem of localization is dealt with by the crack bandwidth parameter. The results are somewhat ambiguous due to the double role played by this param-

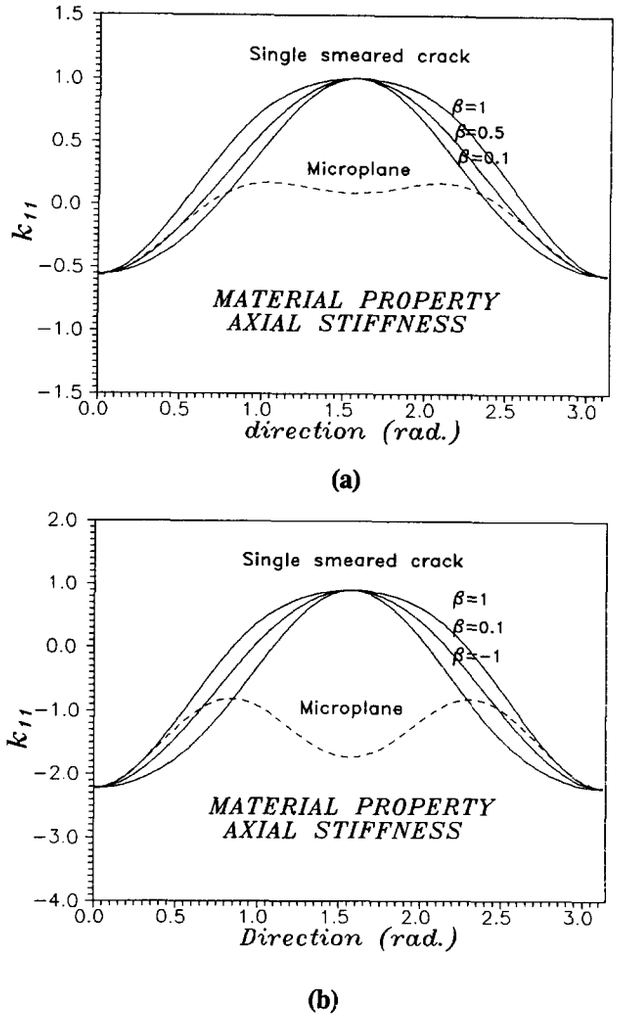

FIG. 2. Variation of Axial Stiffness as a Function of Crack Orientation, for Single Fixed Smeared Crack Approach and for Microplane Material Model: (a) ($\mu = -0.5$); (b) ($\mu = -2$)

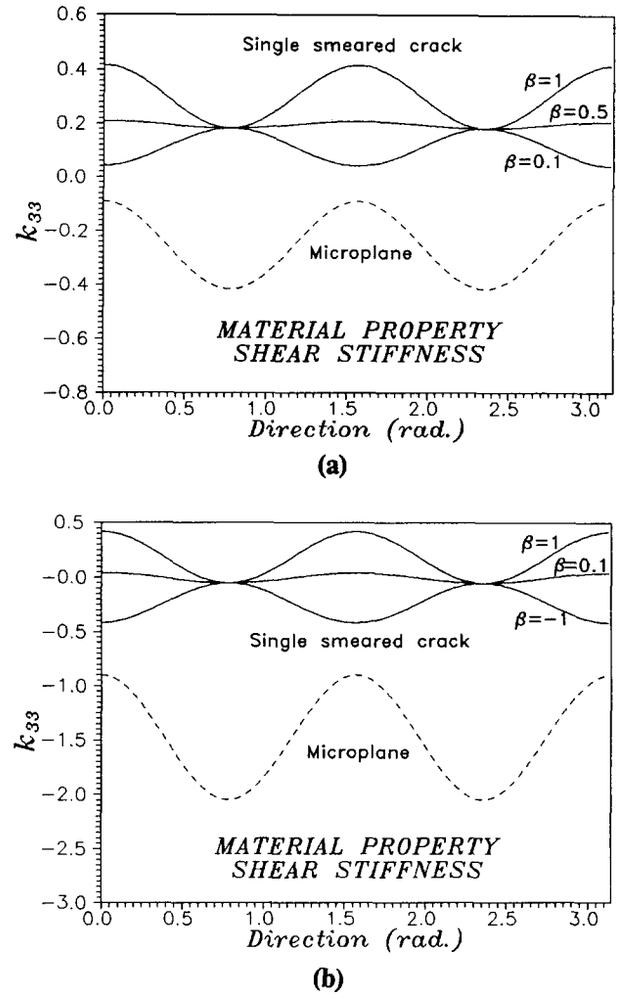

FIG. 3. Variation of Shear Stiffness as a Function of Crack Orientation, for Single Fixed Smeared Crack Approach and for Microplane Material Model: (a) ($\mu = -0.5$); (b) ($\mu = -2$)

eter. The physical correspondent of the crack bandwidth should be the dimension in which damage is expected to take place. This means that if the typical mesh element dimension is smaller than the bandwidth, the fracture energy should be increased to account for the full energy of the band when damage tends to concentrate in one row of elements. However, to smooth out the problem of stress locking, in some finite-element codes the energy-consumption capacity of the element is scaled down to the ratio of the element dimension over the bandwidth. This helps when the mixed mode fracture tends to spread out of control due to the stress locking in shear. In other words, the crack bandwidth is related to the expected spread of damage in the finite-element mesh. The bigger the band, the smaller the energy of the single element. Used in this way, the crack bandwidth parameter tends to be extremely variable, depending on the finite-element configuration instead of being related to the material property.

In the engineering practice most of the finite-element codes in use are based on the local continuum approach. However, there is much evidence that the local finite-element codes, based on the crack band approach, cannot always correctly simulate brittle failure in concrete structures, i.e., strong mesh sensitivity can be observed (de Borst 1991; Ožbolt and Eligehausen 1991). Therefore, the more general nonlocal approaches, which are conceptually multicrack-oriented, have been recently developed and implemented into the finite-element codes. According to the nonlocal concept, the stress at a point depends not only on the strain at the same point, but also on the strain field in a certain neighborhood of the point (Eringen and Edelen 1972). Currently, a few different variations of the concept exist. The most recent one (Bažant 1994) is not a poor mathematical device, which serves to avoid the localization of damage into a zero volume, but it has its physical ground in microcrack interactions. The concept has been coupled together with the microplane material model and implemented into the finite-element code (Ožbolt and Bažant 1994). Some results obtained using this code will be shown later.

COMPARISON: FIXED CRACK AND MICROPLANE MODEL

The previously described material models will be numerically investigated and compared here. Since it is not possible to grasp the behavior of these models in closed (analytical) form, numerical analysis is needed. This, however, cannot be done using the finite-element analysis because in such a case there are too many factors that contribute to the result, thus making it very difficult to distinguish between the role played by each of them. Even at the material level some basic assumptions need to be made in order to make the results clear and generally valid. Bearing this in mind, two small computer codes have been written that assemble the multicrack and the microplane material models.

In the single and multicrack models, the number and ori-

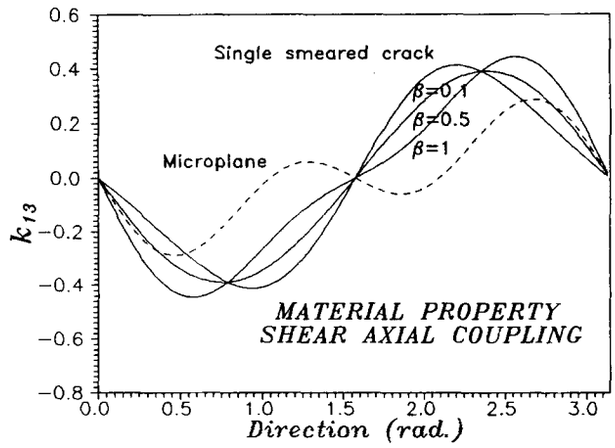

(a)

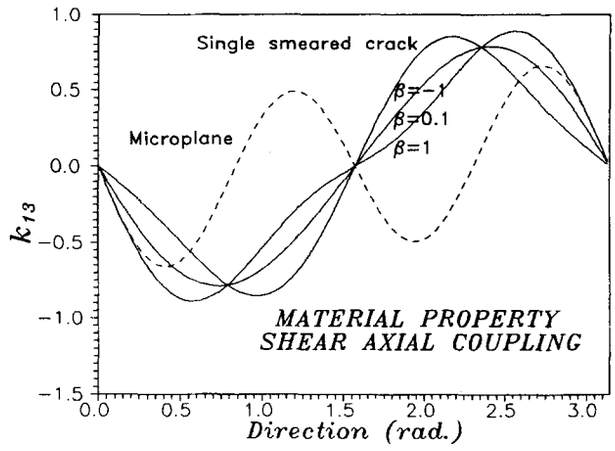

(b)

FIG. 4. Axial-Shear Coupling as a Function of Crack Orientation, for Single Fixed Smeared Crack Approach and for Microplane Material Model: (a) ($\mu = -0.5$); (b) ($\mu = -2$)

entation of planes as well as the crack parameters μ and β for each of them are input data. The tangent stiffness matrix is assembled based on (6). Properties of this matrix are then investigated by varying the orientation of the crack plane/planes [angle α in Fig. 1(a)] with respect to the reference system axis. In the program simulating the microplane material model, global strain history as well as all the material parameters are given by the input. From the global strain increments, the microplane strain increments are calculated using (10). The corresponding stress increments are then obtained with (11)–(14) and macroscopic stress increments are calculated according to (15). The material tangent stiffness matrix on the macrolevel is then found using (17) and (18). The same as for the smeared crack model, properties of this matrix are investigated by rotating the orientation of the local reference system, which coincide with the principal strain axis, with respect to a global reference system. Due to the complexity of both models, the following assumptions are adopted. The initial tangent value for C_N^0 and C_T^0 in the microplane model are chosen to obtain the same initial elastic plane stress stiffness matrix as in the crack approach, with Young's modulus $E = 1$ and Poisson's ratio $\nu = 0.2$. Other values are fixed as $e_1 = 0.00001$, $e_2 = 0.0002$, $k = 1$, and $r = 1.5$.

Criteria for comparing the two models are set as follows. For the single and multiple crack approaches the material damage configuration is fixed in advance in the principal strain direction [see Fig. 1(a)]. This is done by feeding the program with the crack plane relative orientations and softening parameters μ and β for each of them. The microplane model is also subjected to uniaxial strain loading in direction n [see Fig. 1(a)]. The material properties are compared when the same stiffness as for the fixed crack approach is achieved in the principal strain direction. The initial study is carried out using the microplane material model and the single fixed crack approach. Two values for the mode-I softening parameter are chosen: $\mu = -0.5$ and $\mu = -2.0$. For each of these, results are plotted for three different shear retention values of β. With $\mu = -0.5$, we have $\beta = 1$, $\beta = 0.5$, and $\beta = 0.1$; with $\mu = -2.0$ the following values are chosen, $\beta = 1$, $\beta = 0.5$, and $\beta = -1$. In this way the influence of both parameters can be investigated.

Fig. 2 shows the variation of the material stiffness in direction $x(k_{11})$ as a function of the angle between the x-axis and principal strain direction, for both models. It can be seen that in the single crack approach there is no correlation between two principal directions, i.e., when the material is damaged in the x-direction, the stiffness in the perpendicular y-direction is

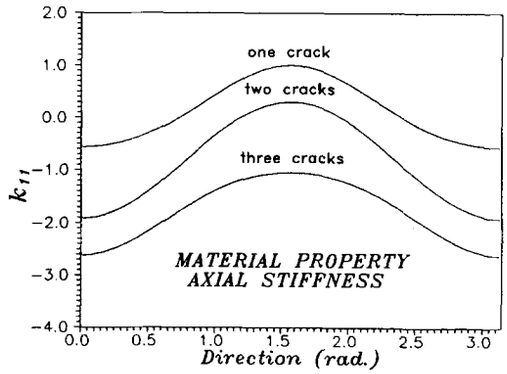

(a)

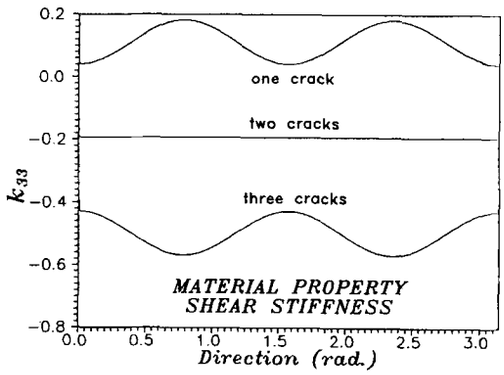

(b)

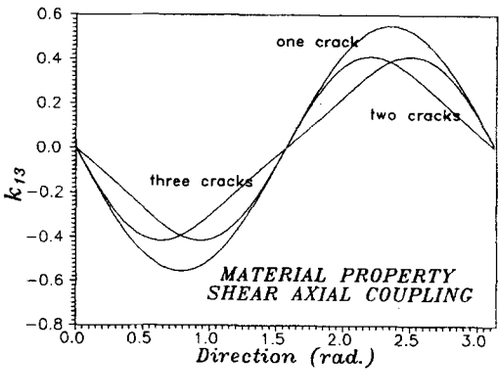

(c)

FIG. 5. Multiple Fixed Crack Approach—Variation of Stiffness as a Function of Crack Orientation for: (a) Axial Stiffness (k_{11}); (b) Shear Stiffness (k_{33}); (c) Axial-Shear Stiffness (k_{13})

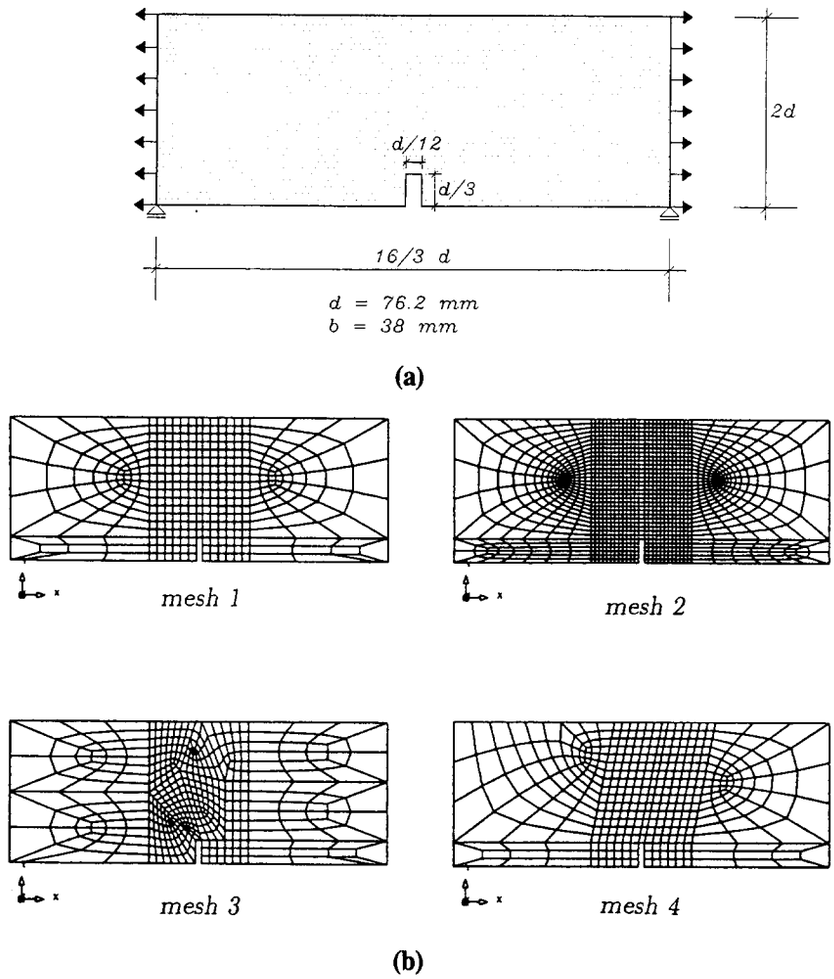

FIG. 6. Eccentric Tension Test: (a) Geometry of Specimen Used in Numerical Case Study; (b) Four Different Finite-Element Meshes Used in Analysis

initially elastic. This is a consequence of the assumption that the shear damage is taking place on the same plane where the mode-I crack opening takes place. According to this assumption the material cracked in one direction, is completely intact on the perpendicular direction. As a matter of fact the tensile strength of a concrete specimen subjected to biaxial tensile strain in two orthogonal directions is almost independent, but this is a structural rather then a material property, thus confirming that the smeared crack models are only fictitiously continuous and do behave instead as discrete models. In contrast to this, in the microplane model the damage develops also on inclined directions, thus providing a correlation between different orientations as expected in a continuous model. The larger the damage in one direction the higher the reduction of the stiffness in the perpendicular direction [compare Figs. 2(a) and 2(b)].

Fig. 3 shows the variation of the shear stiffness (k_{33}) as a function of the crack orientation. It can be seen that the single smeared crack model, compared with the microplane model, overestimates the shear stiffness independently on the β-value, i.e., for $\alpha = 45°$, the shear stiffness is the same for all β-values. For the microplane model the shear stiffness reaches the minimum value at $\alpha = 45°$, the same as for the crack band model with $\beta = 1$. This is due to the joint action of shear damage on this orientation and of reduced axial stiffness on the principal direction. The result is that the principal tensile direction is always a direction of the maximum shear stiffness and rotation of the principal strain does not rebuild stresses as much as in the single crack approach.

The curves for the single crack model clearly show the inconsistency of the shear damage mechanism on the crack plane. When β is set to one, the shear stiffness is strongly overestimated but it shows at least a minimum at $\alpha = 45°$. This seems reasonable since maximum shear strains should be inclined 45° to the principal tensile strain. When β is reduced, even if resulting shear stiffness is decreased, the function (see Fig. 3) exhibits a minimum for $\alpha = 0$ and a maximum at 45°. This is the reason why these models are very sensitive to β, and as soon as its value is not set to zero they rebuild stresses by shear.

Generally, shear component transformation functions have only half of the period of axial ones (90° instead of 180°). This means that the shear damage in the single smeared crack approach cannot be modeled properly as long as shear behavior is specified on one plane only. The reason for defining the shear retention factor on the crack plane must be found again in the discrete crack concepts. When the crack plane is understood to be the plane of the macrocrack the shear capacity is reduced as a result of the physical material gap between the surfaces of the crack.

Fig. 4 shows the axial shear stiffness coupling (k_{13}) as a function of the crack orientation. The microplane material model curve shows a 90° period, as expected from the shear behavior, compared to 180° in the single smeared crack. Again, the curve for $\beta = 1$ seems to approximate the microplane model behavior better than any other value. It is also seen that in the single smeared crack, the function does not change the sign in the 90° sector and is always greater than

in the microplane model, where it does change the sign. This means that the single approach can easily enforce axial stresses via shear deformations (shear locking) and vice versa.

Furthermore, the multiple fixed crack approach is investigated. The same property of the material stiffness matrix as in the previous study are plotted in Fig. 5. The stiffness matrix is assembled with one, two, and three cracks at 45° from each other. The same crack stiffness parameters are used for all the cracks with $\mu = -0.5$ and $\beta = 0.1$. In Fig. 5(a) the axial stiffness (k_{11}) is plotted as a function of the crack orientation. Because the material assembly relys on a series assumption, the resulting stiffness decreases dramatically at the new crack opening even in the case where the angle between the crack is as wide as 45°. When three cracks are active, for a total angle of 90°, the resulting stiffness shows a smoother profile and some correlation between perpendicular directions, i.e., compared with the single crack approach the shear stiffness in perpendicular direction is more reduced. Shear stiffness and shear axial coupling is plotted in Figs. 5(b) and 5(c). The plots show that the new crack openings do not overcome the problem found in the single crack model until the angle spread is large enough for some interaction of different crack directions. Conversely, when the angle between the cracks in small, the resulting stiffness drops significantly with sudden steps at the crack opening, which seems to lack any physical meaning.

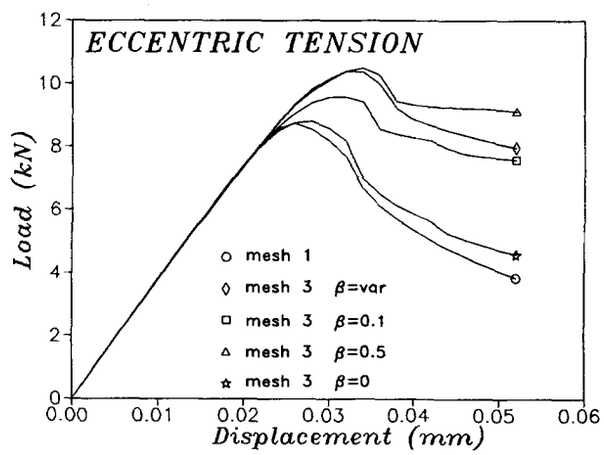

(a)

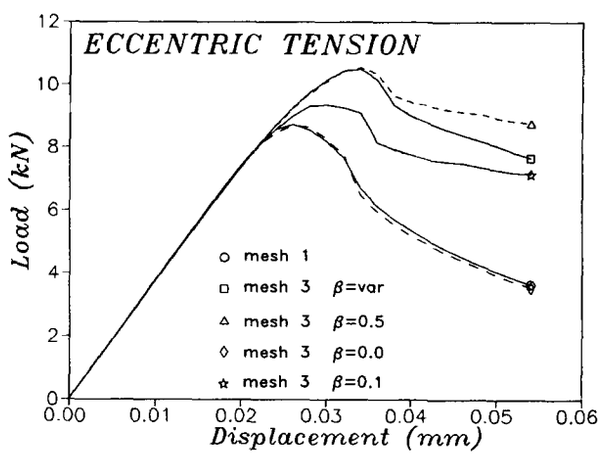

(b)

FIG. 7. Eccentric Tension—Load-Displacement Curves for Different Meshes: (a) Single Fixed Crack Approach; (b) Multiple Fixed Crack Approach

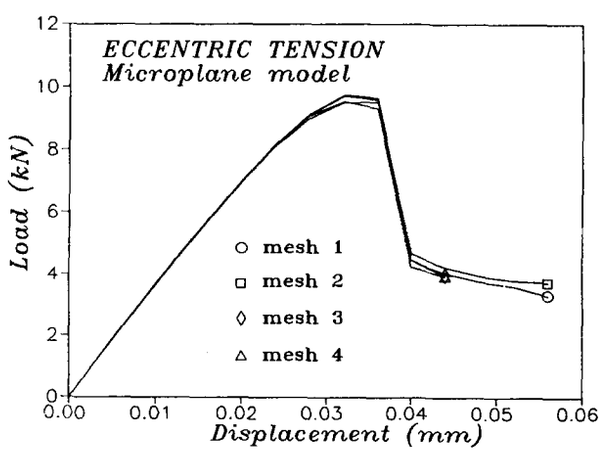

FIG. 8. Eccentric Tension—Load-Displacement Curves for Different Meshes Obtained Using Nonlocal Microplane Model

NUMERICAL CASE STUDIES

The first analyzed example is eccentric tension on a notched specimen under the plane stress assumption. In Fig. 6(a) the geometry of the specimen, boundary, and loading conditions are plotted. The specimen is loaded such that the symmetric failure mode in eccentric tension is enforced by fixing vertical displacement at the bottom edges. The finite-element meshes used in the study are shown in Fig. 6(b). Four node quadrilateral elements with four integration points are used. The microplane material model parameters have been chosen such that the material behavior on the local level yields the uniaxial tensile and compressive strength, $f_t = 2.5$ MPa and $f_c = 34.5$

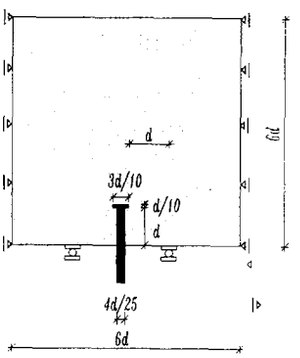

(a)

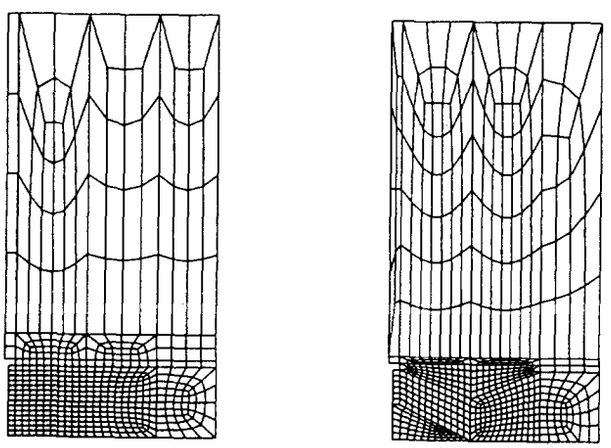

mesh 1 (b) mesh 2

FIG. 9. Pull-Out Test: (a) Geometry of Specimen Used in Numerical Case Study; (b) Two Different Meshes

MPa. Young's modulus and Poisson's ratio are set to 27,000 MPa and 0.18, respectively (Ožbolt and Bažant 1994).

The analysis is carried out using the single and multiple crack approaches with different shear retention factors and crack bandwidths for meshes 1 and 3. The nonlinear mode-I strain-softening branch was adopted according to Reinhardt (Reinhardt et al. 1986; de Witte 1988). Tensile strength was chosen as f_t = 3.0 MPa, Young's modulus and Poisson's ratio as E = 27,000 MPa and ν = 0.18. Fixed and variable shear retention factors are used; variable one according to the expression: $\beta = 1/(1 + 4{,}447\varepsilon_n^{cr})$ (de Witte 1988). Fracture energy is set to G_f = 0.1 N/mm, the crack bandwidth is chosen as C_w = 9 mm with a typical element side dimension in the fracture zone of l = 6.35 mm. The analysis is carried out using the *DIANA* finite-element package.

The load-displacement curves for single crack approach with variable and fixed shear retention factors are plotted in Fig. 7(a). Strong mesh sensitivity can be observed independent of the shear criteria used. In these cases, the mesh shape sensitivity is proportional to the shear retention factor on the crack plane since it causes rebuilding of the tensile stresses in directions other than the direction of the crack. The results for the symmetric mesh are independent of the shear criteria used.

The same examples are analyzed using the multiple crack approach. The threshold angle for the new crack opening is fixed to 5°. Constant and variable shear retention factors are used. The results shown in Fig. 7(b) still exhibit large differences, even if they are slightly smaller than in the single crack approach. The results for mesh 1 are independent of the shear criteria and coincide with the single crack ones.

Fig. 8 shows the load-displacement response obtained for four meshes using the microplane material model together with the nonlocal microcrack interaction approach (Ožbolt and Bažant 1994). As can be seen, there is no significant influence of the mesh shape and size on the load-displacement response.

The example in which mixed mode fracture occurs is further analyzed using the nonlocal microplane model and the single multiple crack approaches. A pull-out test in plane stress, with geometry loading and boundary conditions [Fig. 9(a)] according to the "Round Robin" specifications (RILEM TC 90-FMA 1992), is analyzed. The microplane material model parameters are chosen such that the material behavior on the local level yields the uniaxial tensile and compressive strength, f_t = 2.97 MPa and f_c = 34.5 MPa. Young's modulus and Poisson's ratio are set to 30,000 MPa and 0.18, respectively. The material parameters used in the fixed multiple crack approach are the same as in previous example, except for Young's modulus, which is set to E = 30,000 MPa and the crack bandwidth fixed to C_w = 20 mm. Two different finite-element meshes used in the analysis are plotted in Fig. 9(b). Four node quadrilateral elements and four point Gaussian quadratures are used. To separate the effect of the mesh shape from the mesh size sensitivity, the element's dimensions in the fracture process zone are kept approximately constant (15 mm square) but its orientation is changed in mesh 2.

The single and multiple crack approaches are tested with different shear-retention factors, the threshold angle for the multiple crack approach being fixed at 5°. The pull-out load-displacement curves for mesh 1, using the different crack approaches, are plotted in Fig. 10(a). The equivalent results for mesh 2 is shown in Fig. 10(b). All analyses are stopped at the 1 mm displacement, whether the peak load is reached or not. In some cases the analysis could have been prolonged much further without the structure showing any sign of final collapse. Numerical problems are found for mesh 1 when using a variable shear-retention factor in the multicrack approach. Differences between the multiple and single crack approaches for the same mesh are small compared to the mesh shape sensitivity between the two meshes (see Fig. 11). When the shear-retention factor is set to zero, the load-displacement curve clearly shows an increase of the structural stiffness following the initial cracking at load levels of 40–50 kN. This behavior is due to the increase in the shear stiffness following the rotation of the principle directions. In contrast to the crack band model, the load-displacement curves for the same pull-out test using the nonlocal microplane material model, plotted in Fig. 12, indicates practically no mesh sensitivity.

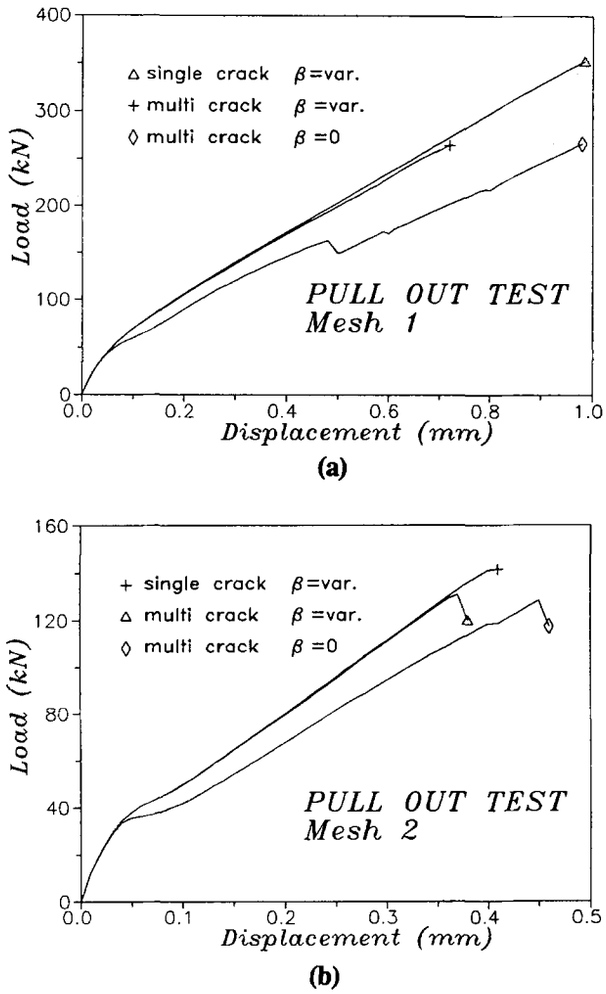

FIG. 10. Pull-Out Test—Load Displacement Curves Obtained Using Fixed Crack Approach for (a) Meshes 1; (b) Mesh 2

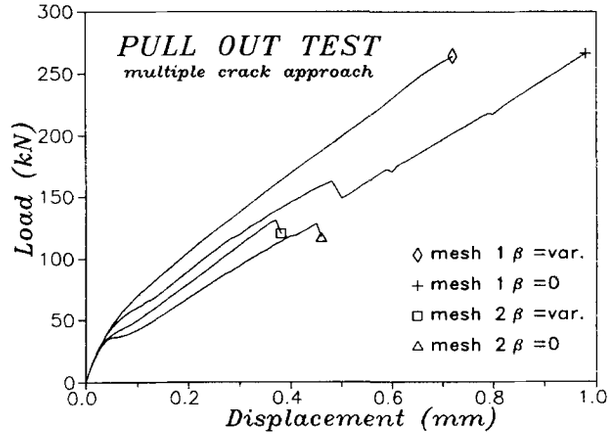

FIG. 11. Pull-Out Test—Load-Displacement Curves Obtained Using Multiple Crack Approach

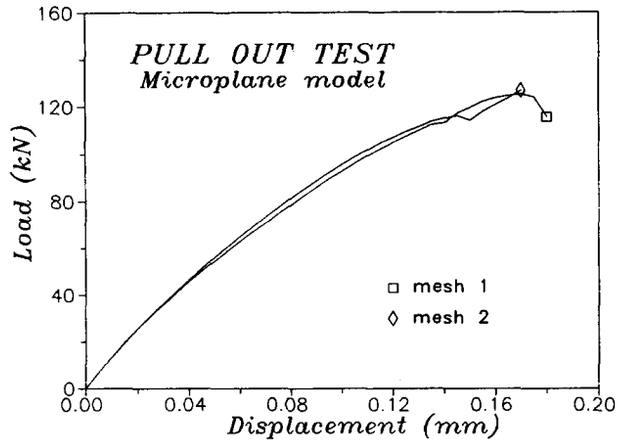

FIG. 12. Pull-Out Test—Load-Displacement Curves Obtained Using Nonlocal Microplane Model

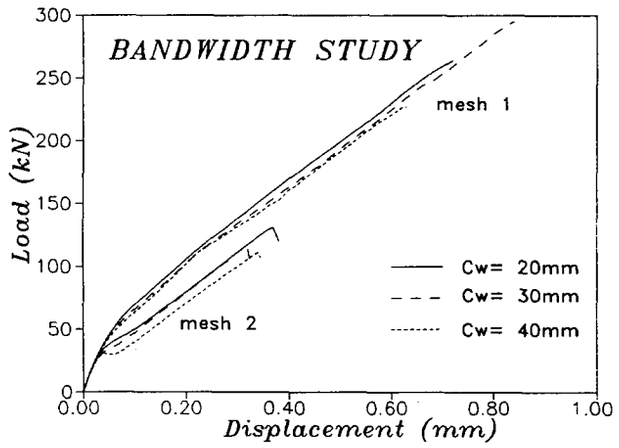

FIG. 13. Crack Bandwidth Study for Meshes 1 and 2 Using Multiple Fixed Crack Approach

The localization limiters are finally tested. For the crack band approach the influence of the crack width is investigated. The foregoing pull-out test is performed with the same parameters except for the crack bandwidth. This is set to C_w = 30 mm and C_w = 40 mm compared to the previously used value of C_w = 20 mm. The multiple crack approach with variable shear-retention factors is tested and results for both meshes are shown in Fig. 13. Since the bandwidth does not have any relation to shear stiffness, effects on mesh 1 are negligible. The influence on the peak load is hard to tell since with C_w = 20 mm, numerical problems were found and the analysis could not be continued; with C_w = 30 mm, the response did not show any softening up to 1.0 mm; and with C_w = 40 mm, snapback occurred and the last converged step is believed to be the peak load. The wider crack bandwidth should generally anticipate the collapse of the model via zero resistance in mode I, but, if the mesh is not following the crack direction, the shear locking provides the required stiffness through rotated stress paths. The results using mesh 2 are more consistent. The initial mode-I mechanism yields different stiffnesses depending on the crack bandwidth. Later, with the activation of the shear mechanism, the structure behaves independently of this parameter as expected from the material model definition.

CONCLUSIONS

Today most finite-element codes for the fracture analysis of concrete structures use the single or multiple crack approach described in the paper. There are of course some variants, but the basic hypothesis and procedure for the stiffness matrix assembly does not seem to differ substantially from the one described. Since the resulting material model of this crack approach is not continuous, it cannot be generally used in the continuous finite-element analysis. The model can be used only bearing in mind that it is still a discrete approach needing careful adaptation of the mesh direction and crack width parameter. Remeshing techniques could be used, the resulting approach being totally equivalent to the discrete crack one.

The nonlocal microplane material model seems to overcome these problems with a completely different concept in the material stiffness matrix assembly. Even using the stress-strain relations defined on planes of various orientations, the three-dimensional behavior is obtained by a kinematic constraint approach and an integration of microplane stresses over the unit volume. This ensures basic continuity in the resulting material model properties.

In recent years the problem of mesh sensitivity has been intensively investigated. Even though many aspects of it are now clear, there is still a well-established opinion that most of these problems are inevitable when softening material behavior must be taken into account. As discussed here, the shear locking and mesh shape sensitivity can be avoided when a consistent material model is used.

APPENDIX. REFERENCES

Bažant, Z. P. (1983). "Comment on orthotropic models for concrete and geomaterials." *J. Engrg. Mech.*, ASCE, 109(3), 849–865.

Bažant, Z. P. (1986). "Mechanics of distributed cracking." *Appl. Mech. Rev.*, Vol. 39, 675–705.

Bažant, Z. P. (1994). "Nonlocal damage theory based on micromechanics of crack interactions." *J. Engrg. Mech.*, ASCE, 120(3), 593–617.

Bažant, Z. P., and Oh, B. H. (1983). "Crack band theory for fracture of concrete." *Mat. and Struct.*, 16(93), 155–177.

Bažant, Z. P., and Prat, P. C. (1988). "Microplane model for brittle-plastic material. Parts I and II." *J. Engrg. Mech.*, ASCE, 114(10), 1672–1702.

Broek, D. (1987). *Elementary engineering fracture mechanics*. Martinus Nijhoff Publishers, Doordrecht, The Netherlands, 77.

Cope, R. J., Rao, P. V., Clarck, L. A., and Norris, P. (1980). "Modelling of reinforced concrete behavior for finite element analysis of bridge slabs." *Numerical methods for nonlinear problems 1*, C. Taylor et al., eds., Pineridge Press, Swansea, Wales, 457–470.

Crisfield, M. A., and Willis, J. (1987). "Numerical comparison involving different 'concrete-models.'" *IABSE Rep. 54*, Coll. Comp. Mech. of Reinforced Concrete, Delft Univ. Press, Delft, The Netherlands, 177–187.

de Borst, R. (1987). "Smeared cracking, plasticity, creep and thermal loading—a unified approach." *Comp. Meth. Appl. Mech. Engrg.*, Vol. 62, 89–110.

de Borst, R. (1991). "Continuum models for discontinuous media." *Proc., Int. RILEM/ESIS Conf. on Fracture Processes in Concrete, Rock and Ceramics*, 601–618.

de Borst, R., and Nauta, P. (1985). "Non-orthogonal cracks in a smeared finite element model." *Engrg. Computations* 2, 35–46.

de Witte, F. C. (ed.) (1988). *DIANA user-manual*. Inst. TNO Inst. for Build. Mat. and Struct., Delft, The Netherlands.

Eringen, A. C., and Edelen, D. G. D. (1972). "On nonlocal elasticity." *Int. J. Engrg. Sci.*, Vol. 10, 233–248.

Ožbolt, J., and Bažant, Z. P. (1992). "Microplane model for cyclic triaxial behavior of concrete." *J. Engrg. Mech.*, ASCE, 118(7), 1365–1386.

Ožbolt, J., and Bažant, Z. P. (1994). "Numerical smeared fracture analysis: nonlocal microcrack interaction approach." *Int. J. Numer. Methods in Engrg.*

Ožbolt, J., and Eligehausen, R. (1991). "Analysis of reinforced concrete beams without shear reinforcement using nonlocal microplane model." *Proc., Int. RILEM/ESIS Conf. on Fracture Processes in Concrete, Rock and Ceramics*, 919–930.

Reinhardt, H. W., Cornelissen, H. A. W., and Hordijk, D. A. (1986). "Tensile test and failure analysis of concrete." *J. Struct. Engrg.*, ASCE, 112(11), 2462–2477.

RILEM TC90-FMA. (1992). "Round-robin analysis of anchor bolts—II." *Fracture mechanics of concrete applications*, Univ. of Lulea, Sweden.
Rots, J. G. (1988). "Computational modeling of concrete structures," PhD dissertation, Delft, The Netherlands.
Rots, J. G. (1992). "Removal of finite elements in strain-softening analysis of tensile fracture." *FramCoS 1*, Z. P. Bažant, ed., Elsevier Applied Science, New York, N.Y., 330–338.
William, K., Bićanić, N., and Sture, S. (1986). "Composite fracture model for strain-softening and localised failure of concrete." *Computational modelling of reinforced concrete structures*, E. Hinton and D. R. J. Owen, eds., Pineridge Press, Swansea, Wales, 122–153.